CONDITIONS OF FRAGMENT FORMATION IN CENTRAL AND PERIPHERAL COLLISIONS

W.F.J. MÜLLER for the ALADIN COLLABORATION

Gesellschaft für Schwerionenforschung (GSI)
Planckstr. 1, D-64291 Darmstadt, Germany

Abstract

We report on new measurements of the breakup temperature determined from isotope ratios as well as from state population ratios for the decay of the spectator in Au + Au collisions at 600 and 1000 A MeV and compare them to results for the decay of the participant region at beam energies of 50 - 200 A MeV. Temperatures deduced from the new isotope thermometer T_{BeLi} exhibit a pronounced rise with increasing excitation energy and are consistent with the previously studied T_{HeLi}. In contrast, temperatures determined from state population ratios show no dependence on excitation energy. An improved calorimetric determination of the excitation energy for the spectator shows a significant increase with increasing bombarding energy which is in contrast to the observed universality of the fragment production.

1 Introduction

The existence of phase transitions in nuclear matter was proposed about 25 years ago in conjunction with the description of the structure of neutron stars [1]. The observation of a power law for the fragment size distribution [2] was a first experimental hint for a second order phase transition. Only the present generation experiments with an almost complete coverage for the decay products finally allow to address the question whether signals of a first or second order phase transition can be observed in the disintegration of highly excited nuclei in a quantitative fashion.

One standard technique for detecting phase transitions is to measure the relationship between the temperature and the excitation energy, known as the caloric curve. Indeed, the caloric curve for excited projectile spectators in Au + Au collisions at 600 A MeV exhibits a shape reminiscent of a first order phase transition in macroscopic systems [4]. There the temperature was determined from a double ratio of isotopic yields [3] and the excitation energy by summing the kinetic energies and the total binding energy of the decay products. This finding stimulated theoretical and experimental studies on the interpretation of the caloric curve [5, 6] and on methodical questions, in particular whether breakup temperatures in the 5-10 MeV range can be reliably determined [7, 8, 9, 10, 11, 12]. The caloric curves for other systems have been reported in addition [13, 14]. In this contribution we focus on how the physical quantities plotted in the caloric curve are experimentally determined. We present new experimental results for isotope thermometers and address the question of pre-breakup contributions to the excitation energy.

2 Breakup Temperatures

The temperatures used in the caloric curve studies [4, 13, 14] were deduced from a double ratio of isotopic yields. Under the assumptions of low density and chemical equilibrium a grand canonical treatment [3] yields for the double ratio of ground state

$$\frac{Y_{(A_1,Z_1)}/Y_{(A_2,Z_2)}}{Y_{(A_3,Z_3)}/Y_{(A_4,Z_4)}} = a\exp\left(\frac{\Delta B}{T}\right) \qquad \text{with} \quad \Delta B = B_1 - B_2 - B_3 + B_4 \quad (1)$$

where a is a statistical factor containing spin and mass terms and B_i represents the binding energy of isotope i. The double ratio is in this approximation independent of the proton and neutron chemical potential if the isotope pairs 1-2 and 3-4 differ both by either one neutron or one proton. Futhermore, for best sensitivity the binding energy difference ΔB should be comparable or larger than the temperatures to be measured [9]. The reliability of temperatures deduced from isotope ratios has been questioned for mainly two reasons:

- The apparent temperatures of Eq. (1) are distorted by sequential feeding from γ-instable states and from particle decay of heavier isotopes. The influence of γ states can be calculated analytically and absorbed in an effective and temperature dependent statistical factor a. In contrast, the effect of particle decay can only be estimated in a model dependent way. A variety of prescriptions have been proposed [7, 8, 10] for the initial composition of the source and the treatment of continuum states, excluded volume effects, and other factors.

- Isotope temperatures reflect the thermodynamic conditions of fragment formation only to the extent that all ejectiles are emitted from the same equilibrated breakup state. If the emission is time ordered, as for example the EES model suggests [15], light charged particles including ^{3}He are emitted on average at an earlier and hotter stage of the expansion than the IMF's . T_{HeLi} consequently reflects the average ^{3}He emission

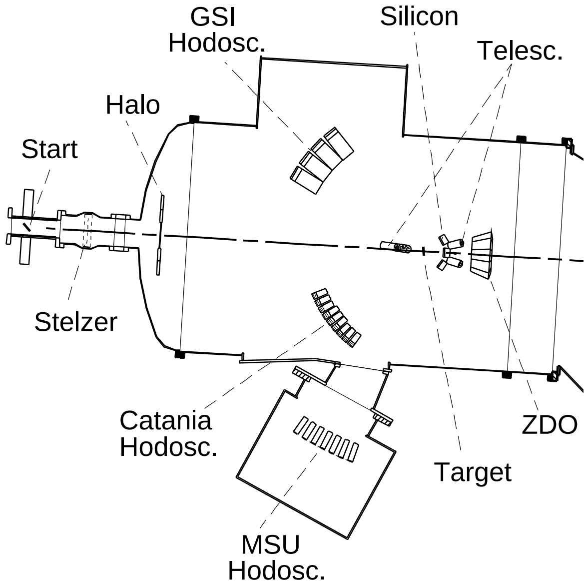

Figure 1: Setup for the study of spectator breakup in semi-peripheral Au + Au reactions at 1000 A MeV.

temperature which is considerably above the temperature where most IMF's are formed.

An experiment was performed at the ALADIN spectrometer at GSI to address both issues by a systematic study of temperatures extracted from various isotope ratios and excited-state population ratios. Spectator breakup was studied for semi-peripheral Au + Au collisions at 1000 A MeV as well as the emission from the participant region in central Au + Au collisions at 50, 100, 150, and 200 A MeV.

The setup for the 1000 A MeV experiment shown in Fig. 1 was optimized to study target spectators. Seven telescopes, each consisting of 3 Si detectors with a thickness of 50, 300, and 1000 μm followed by a 4 cm CsI(Tl) scintillator, were used to measure isotopic yields and spectral shapes. Three large area Si-CsI hodoscopes with high granularity, placed at 135°, allowed to determine the yield of particle unstable states from light charged particle correlations. The decay products of the projectile spectator were detected in the time-of-flight wall of the ALADIN forward spectrometer [16] and, exploiting the symmetry of the reaction, used for the event characterization. This minimized auto-correlations with the observables determined from the target spectator products.

The setup for 50-200 A MeV was similar, but had the hodoscopes placed at forward angles covering the region around 90° in the cm-system, thus minimizing the contribution from projectile and target fragmentation.

T_x	Isotope Ratio	a	ΔB (MeV)
$T_{\rm Hepd}$	$\frac{^1\mathrm{H}/^2\mathrm{H}}{^3\mathrm{He}/^4\mathrm{He}}$	5.51	18.35
$T_{\rm Hedt}$	$\frac{^2\mathrm{H}/^3\mathrm{H}}{^3\mathrm{He}/^4\mathrm{He}}$	1.59	14.32
$T_{\rm HeLi}$	$\frac{^6\mathrm{Li}/^7\mathrm{Li}}{^3\mathrm{He}/^4\mathrm{He}}$	2.18	13.33
$T_{\rm tHeLiBe}$	$\frac{^6\mathrm{Li}/^7\mathrm{Be}}{^3\mathrm{H}/^4\mathrm{He}}$	2.18	14.21
$T_{\rm BeLi}$	$\frac{^9\mathrm{Be}/^8\mathrm{Li}}{^7\mathrm{Be}/^6\mathrm{Li}}$	1.76	11.28
$T_{\rm CLi}$	$\frac{^6\mathrm{Li}/^7\mathrm{Li}}{^{11}\mathrm{C}/^{12}\mathrm{C}}$	5.90	11.47
$T_{\rm CC}$	$\frac{^{12}\mathrm{C}/^{13}\mathrm{C}}{^{11}\mathrm{C}/^{12}\mathrm{C}}$	7.92	13.77

Table 1: Summary of isotope ratio thermometers studied in this contribution. a and ΔB are the statistical factor and the binding energy difference in Eq. (1).

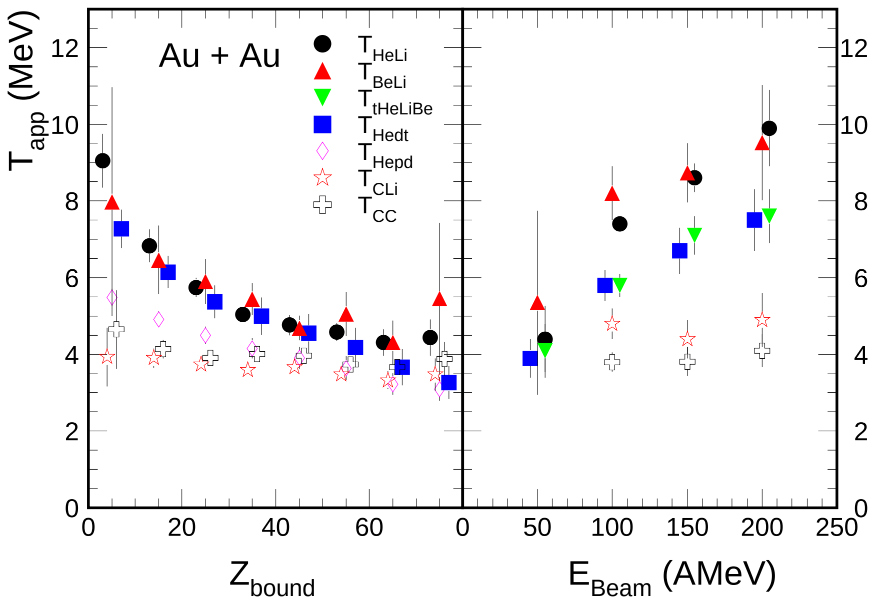

Figure 2: Apparent temperatures deduced from isotope ratios for spectator decay (left panel) and emission from the participant zone (right panel) in Au + Au collisions as a function of $Z_{\rm bound}$ or $E_{\rm beam}$, respectively (From Ref. [17]).

The apparent temperatures for seven different isotope combinations (see Table 1) are summarized in Fig. 2. The left panel shows the results for spectator decay as a function of $Z_{\rm bound}$, which is defined as the sum of all spectator charges with $Z \geq 2$ and is closely correlated with the excitation energy deposited in the early stage of the reaction. $T_{\rm Hepd}$ and $T_{\rm Hedt}$ were deduced from target spectator data at 1000 A MeV while $T_{\rm HeLi}$, $T_{\rm BeLi}$, $T_{\rm CLi}$, and $T_{\rm CC}$ were deduced

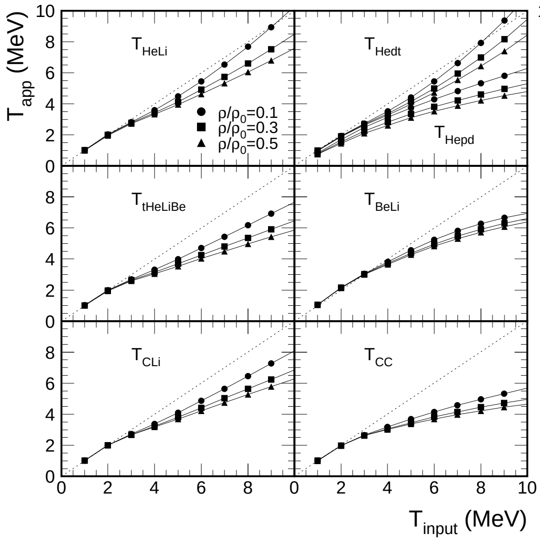

Figure 3: Apparent temperatures determined from the isotope distributions calculated with the QSM model as a function of the model input temperature T_{input} for different breakup densities ρ/ρ_0 (From Ref. [17]).

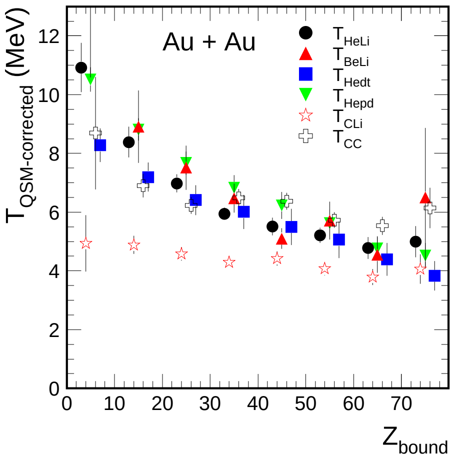

Figure 4: Feeding corrected isotope temperatures for spectator decay in Au + Au collisions. The correction is based on a QSM calculation with a breakup density of $\rho/\rho_0 = 0.3$ (From Ref. [17]).

from projectile spectator data at 600 A MeV. The results for the participant zone in central collisions is presented in the right panel. In both cases T_{HeLi}, T_{BeLi}, and T_{Hedt} exhibit a significant increase with excitation energy, which increases with decreasing Z_{bound} and is roughly proportional to E_{beam}. In contrast, thermometers based on the $^{11}C/^{12}C$ isotope pair show very little Z_{bound} or E_{beam} dependence.

The effect of feeding was estimated with the QSM model [18, 19]. The relation between initial and apparent temperatures is fairly linear for T_{HeLi} but saturates for example for T_{CC} (Fig. 3). The sensitivity on the assumed breakup density is relatively small in all cases. The QSM corrected temperatures are summarized in Fig. 4. All three temperatures based on the $^3He/^4He$ isotope pair give, within error bars, a consistent picture. More importantly, the T_{BeLi} thermometer follows this trend, indicating that the observed rise is not caused by specific properties of the $^3He/^4He$ isotope pair.

An alternative method to determine temperatures is to evaluate the population ratio of two states in one isotope. This type of thermometer reproduces the expected temperatures in compound nucleus reactions at low excitation

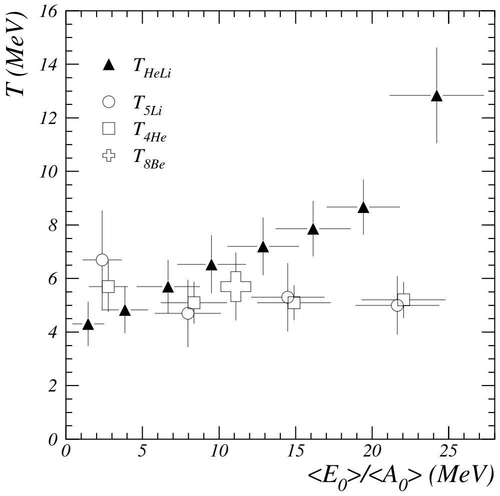

Figure 5: Isotope temperature T_{HeLi} (full triangles) and excited-state temperatures (open symbols) as a function of the excitation energy per nucleon $\langle E_0\rangle/\langle A_0\rangle$ for spectator breakup in the reaction Au + Au at 1000 A MeV. The value of T_{8Be} represents an average over the full range of $\langle E_0\rangle/\langle A_0\rangle$ (From Ref. [20]).

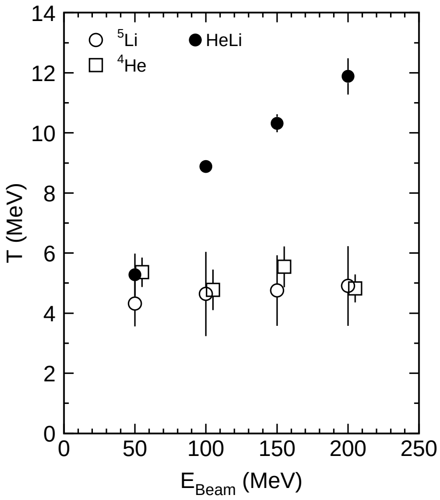

Figure 6: Comparison of T_{HeLi} (full dots) with excited-state temperatures (open symbols) as a function of beam energy for the decay of the participant zone in the reaction Au + Au (From Ref. [21]).

energies, but a large body of experimental evidence shows that there is only a very weak dependence of the temperature for higher excitation energies [22].

The temperatures deduced from population ratios of states in ^{4}He (g.s.; group of 3 states at 20.21 MeV and higher), ^{5}Li (g.s.; 16.66 MeV) and ^{8}Be (3.04 MeV; group of five states at 17.64 MeV and higher) are compared with T_{HeLi} for spectator decay and emission from the participant zone in central collisions in Fig. 5 and 6, respectively. The observed excited-state temperatures are essentially independent of the excitation energy and center around 5 MeV, in striking contrast to T_{HeLi}.

3 Excitation Energy

The excitation energy scale used in the caloric curve was determined by summing up the kinetic energies and the total binding energy of the decay products. This calorimetric method [23] requires in principle the complete knowledge of

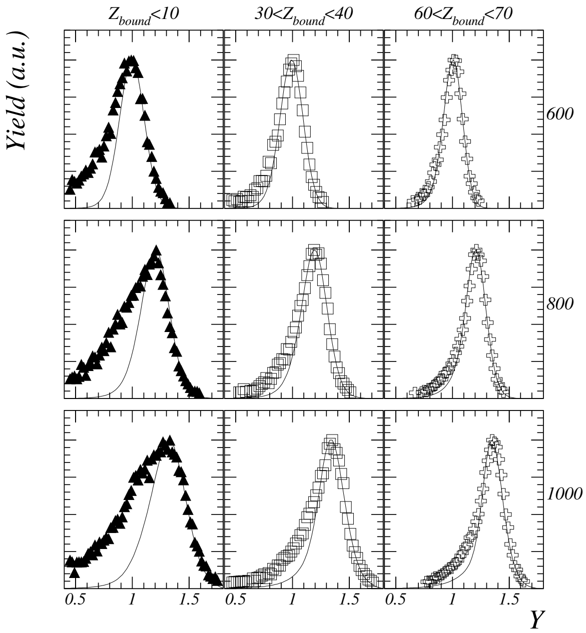

Figure 7: Rapidity spectra of neutrons for three bins in Z_{bound} for the reaction Au + Au at 600, 800, and 1000 A MeV for a cut in transverse momentum of 35 MeV/c $\leq p_t \leq$ 70 MeV/c. The line represents the fit of a gaussian distribution to the $y \geq y_{\mathrm{proj}}$ part of the distribution (From Ref. [20]).

the exit channel. For the Au + Au reaction at 600 A MeV studied in [4] the multiplicity and kinetic energy of the neutrons from projectile spectator decay was measured with the LAND detector. On the other hand, hydrogen isotopes were not detected and their multiplicity was estimated based on assumptions about the N/Z ratio of the spectator and the p/d/t ratio. The mean kinetic energy was assumed to be the neutron kinetic energy plus a Coulomb contribution.

The data for hydrogen emission from the target spectator for the Au + Au reaction at 1000 A MeV, taken with the backward angle telescopes of the present experiment, combined with the neutron data for the projectile spectator at 600, 800 and 1000 A MeV give now a much more complete picture of the light particle emission. The rapidity distribution for the neutrons with a p_t between 35 and 70 MeV/c is shown in Fig. 7 for the three investigated beam energies and three Z_{bound} cuts. Even though the low p_t cut reduces contributions from quasi-free scattering one observes a component in the range between projectile and mid-rapidity which strongly increases in intensity with decreasing Z_{bound}. To suppress this pre-equilibrium component the neutron multiplicity was derived from a fit of a gaussian to the $y \geq y_{\mathrm{proj}}$ part of the distribution (full line in Fig. 7). Because of the substantially better resolution the mean kinetic energy of the neutrons was derived from the transverse momentum distribution of the $y \geq y_{\mathrm{proj}}$ part (Fig. 8). The mean kinetic energy increases not

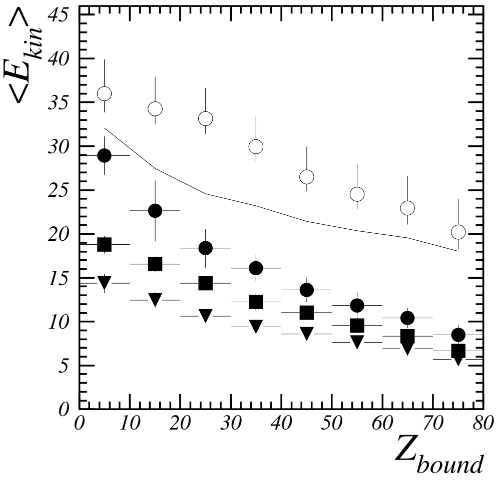

Figure 8: Mean kinetic energy of neutrons (full symbols) in the rest frame of the projectile spectator for the reaction Au + Au at 600 (triangles), 800 (squares), and 1000 A MeV (circles). For E/A = 1000 MeV, the measured mean kinetic energies of protons (open circles) are shown in comparison to the sum of the neutron kinetic energies and an estimated Coulomb contribution (full line, from Ref. [20]).

only with decreasing $\mathrm{Z_{bound}}$ but also significantly with increasing beam energy, a trend also clearly visible in the longitudinal width (Fig. 7). Also shown in Fig. 8 is the mean kinetic energy measured for protons at 1000 A MeV which is significantly higher than the previously used estimate.

The new estimate for the average excitation energy $\langle E_0 \rangle / \langle A_0 \rangle$ of the decaying spectator is presented in Fig. 9. It is based on the combined neutron and proton data and the assumption that the proton energies scale with E_{beam} like the neutron energies. The observed beam energy dependence of $\langle E_0 \rangle / \langle A_0 \rangle$ is in sharp contrast to the beam energy independence of the fragment production [16], which allowed to reproduce fragment multiplicities and charge correlations with statistical multifragmentation models using a single relation between excitation energy and source mass (full line in Fig. 9, see [20, 24]).

4 Summary

The primary goal of the presented study was to check the temperature and excitation energy scale used in the caloric curve.

The investigated isotope temperatures exhibit a consistent picture for spectator decay and emission from the participant zone. The $\mathrm{T_{BeLi}}$ thermometer shows the same increase with excitation energy as the thermometers based on the ^{3}He/^{4}He isotope pair. $\mathrm{T_{BeLi}}$ should be much less susceptible to the emission time order effects discussed for the ^{3}He/^{4}He pair [15, 25] and suffers less from particle and γ feeding than the ^{11}C/^{12}C based thermometers. Currently, $\mathrm{T_{BeLi}}$ seems to be the best candidate for a robust thermometer for the determination of the chemical freeze-out temperature.

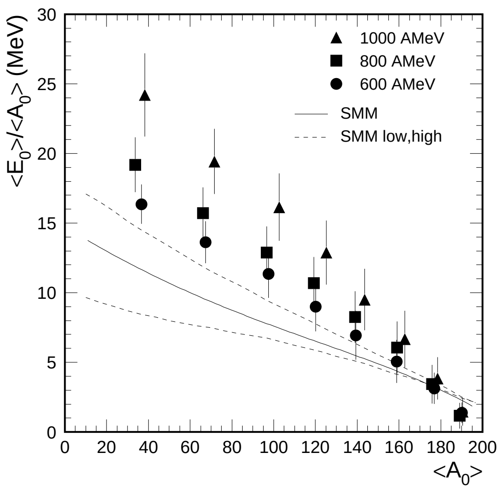

Figure 9: Mean excitation energy per nucleon as a function of the spectator mass $\langle A_0 \rangle$ for the reaction Au + Au. The full line indicates the excitation energy which reproduces the observed fragment distributions in a statistical model calculation, the dashed lines give upper and lower limits (From Ref. [20]).

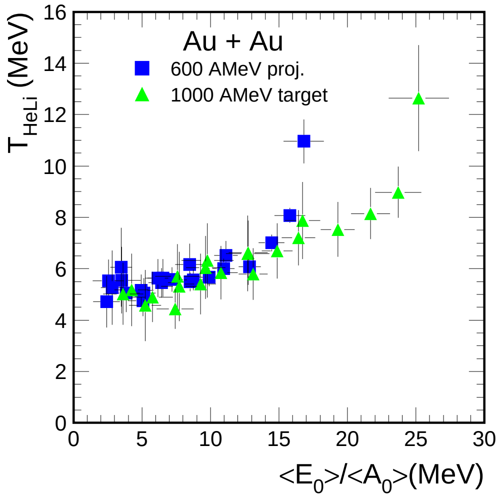

Figure 10: Caloric curve for spectator decay in Au + Au collisions at 600 and 1000 A MeV. The temperature was determined from projectile spectators at 600 A MeV and from target spectators at 1000 A MeV (From Ref. [17]).

In contrast to the isotope thermometers the excited-state thermometers show no dependence on excitation energy but stay at about 5 MeV. Whether this difference is a sign of different freeze-out conditions for the chemical and internal degrees of freedom or an indication that fragment formation is a non-equilibrium process, as QMD suggests [26], remains to be seen.

The observed beam energy dependence of the excitation energy scale is consistent with the picture that a significant and with initial energy deposition increasing fraction of the light particles is emitted prior to the final breakup stage. The present approach in calorimetry yields a caloric curve which depends on beam energy (Fig. 10), clearly at variance with a simple thermodynamical interpretation. A better experimental separation of the pre-equilibrium and pre-breakup contributions in light particle emission is therefore one of the central questions currently being addressed in a study of the C + Au reaction over a wide range of bombarding energies with the INDRA detector at GSI.

References

[1] R.G. Palmer and P.W. Anderson, Phys. Rev. D **9** (1974) 3281.

[2] J.E. Finn *et al.*, Phys. Rev. Lett. **49** (1982) 1321.

[3] S. Albergo *et al.*, Il Nuovo Cimento **89A** (1985) 1.

[4] J. Pochodzalla *et al.*, Phys. Rev. Lett. **75** (1995) 1040.

[5] J.B. Natowitz *et al.*, Phys. Rev. C **52** (1995) R2322.

[6] L.G. Moretto *et al.*, Phys. Rev. Lett. **76** (1996) 2822.

[7] M.B. Tsang *et al.*, Phys. Rev. C **53** (1996) R1057.

[8] Hongfei Xi *et al.*, Phys. Rev. C **54** (1996) R2163.

[9] M.B. Tsang *et al.*, Phys. Rev. Lett **78** (1997) 3836.

[10] F. Gulminelli and D. Durand, Nucl. Phys **A615** (1997) 117.

[11] Z. Majka *et al.*, Phys. Rev. C **55** (1997) 2991.

[12] Hongfei Xi *et al.*, Phys. Rev. C **58** (1998) R2636.

[13] J.A. Hauger *et al.*, Phys. Rev. Lett. **77** (1996) 235.

[14] Y.-G. Ma *et al.*, Phys. Lett. **B390** (1997) 41.

[15] W. Friedmann, contribution to this conference

[16] A. Schüttauf *et al.*, Nucl. Phys. **A607** (1996) 457.

[17] T. Odeh, PhD thesis, Universität Frankfurt (1999).

[18] D. Hahn and H. Stöcker, Nucl. Phys. **A476** (1988) 718.

[19] J. Konopka *et al.*, Phys. Rev. C **50** (1994) 2085.

[20] C. Groß, PhD thesis, Universität Frankfurt (1998).

[21] V. Serfling *et al.*, Phys. Rev. Lett. **80** (1998) 3928.

[22] C. Schwarz *et al.*, Phys. Rev. C **48** (1993) 676.

[23] X. Campi *et al.*, Phys. Rev. C **50** (1994) R2680.

[24] Hongfei Xi *et al.*, Z. Phys. A **359** (1997) 387.

[25] R. Bougault, contribution to this conference

[26] J. Aichelin, contribution to this conference